Journal of Molecular Structure 1356 (2026) 145125

Contents lists available at ScienceDirect

Journal of Molecular Structure

journal homepage: www.elsevier.com/locate/molstr

Effect of glass fiber on rheological, thermal and mechanical properties of EPDM composites

Gizem Halitoğulları [a], İlker Köprü [b], Sinan Köse [c], Fatma Ulusal [d], Salih Hakan Yetgin [e,*]

[a] Tarsus University, Faculty of Engineering, Department of Industrial Engineering, Tarsus, Turkey
[b] Seçil Kauçuk San. Ve Tic. Ltd. A.Ş., Tarsus, Turkey
[c] Ordu University, Fatsa Faculty of Marine Sciences, Department of Naval Architecture and Marine Engineering, Fatsa, Turkey
[d] Tarsus University, Mersin Tarsus Organized Industrial Zone Technical Sciences Vocational School, Department of Chemistry and Chemical Processing Technologies, Tarsus, Turkey
[e] Tarsus University, Faculty of Engineering, Department of Mechanical Engineering, Tarsus, Turkey

ARTICLE INFO

Keywords:
Glass fiber
EPDM
Crosslink density
Mechanical properties
Rheological properties

ABSTRACT

The development of high-performance filled rubber composites has opened a new era in industrial polymer research. In this study, the effects of glass fiber (CE) on the rheological behavior, crosslink density, mechanical performance, thermal characteristics, and morphology of ethylene-propylene-diene monomer (EPDM) rubber composites were investigated. EPDM composites filled with CE at loadings of 11, 22, 54, 90, and 145 phr were prepared using a laboratory-type Banbury mixer and subsequently vulcanized by compression molding to obtain test specimens. It was observed that the CE was homogeneously distributed in the EPDM rubber. The tensile modulus increased by 19.7% with increasing CE content. The tensile strength reached a maximum value of 12.1 MPa at 22 phr CE content, after which a decline was observed. The addition of CE to the EPDM rubber led to an increase in both minimum torque (ML) and maximum torque (MH) values while reducing the scorch time (t_{s2}) and curing time (t_{90}). Furthermore, the crosslink density increased by 429% with the addition of CE. As a result of the study, it is evaluated that CE can be an alternative material for the production of EPDM composites with high temperature resistance and improved mechanical and physical properties.

1. Introduction

EPDM rubber, first introduced into commercial production in the United States in 1963, was developed as an extension of ethylene-propylene rubber (EPM). EPM is a saturated copolymer produced through the copolymerization of ethylene and propylene monomers, and it can be crosslinked by means of peroxides or radiation. Unlike EPM, EPDM incorporates a third monomer into its molecular backbone, which enables vulcanization not only with peroxides and radiation but also with sulfur-based curing agents. The diene component of EPDM is generally selected from one of three types: 2-ethylidene-5-norbornene (ENB), dicyclopentadiene (DCPD), or 1,4-hexadiene (1,4-HD). Among these, ENB is preferred in most commonly used because of its superior performance characteristics. In terms of composition, EPDM typically contains about 45–80 % ethylene, 20–40 % propylene, and 1–12 % of a non-conjugated diene. The physical behavior of the polymer is strongly influenced by the ethylene-to-propylene ratio. For example, a lower ethylene content of 45–50 % leads to an amorphous structure, whereas a higher level, in the range of 70–80 %, contributes to partial crystallinity and the formation of extended molecular chains [1–5]. Due to the saturated backbone structure of its polymer chain, EPDM rubber provides outstanding resistance against environmental aging factors such as oxygen, ozone, and ultraviolet radiation. Its high capacity to absorb fillers and processing oils also facilitates the development of cost-efficient rubber formulations. In addition, EPDM shows notable resistance to both aqueous solutions and concentrated acids and bases, while its relatively low density contributes to the manufacture of lightweight components. The material further possesses advantageous dielectric characteristics, which broaden its applications to products such as sealing profiles, gaskets, hoses, and conveyor belts [6–7]. On the other hand, the material's limited thermal endurance—generally up to around 130 °C—together with its comparatively weak dynamic and mechanical performance, constrains its use in more demanding or specialized fields [8]. In engineering applications, the most commonly

* Corresponding author.
E-mail address: shakanyetgin@tarsus.edu.tr (S.H. Yetgin).

https://doi.org/10.1016/j.molstruc.2025.145125
Received 6 October 2025; Received in revised form 25 November 2025; Accepted 20 December 2025
Available online 20 December 2025

adopted approach to enhance the final performance of rubber components is the incorporation of fillers. Among these, carbon black (CB) and silica are the most widely used. Khalaf [9] reported that increasing the SiO_2 concentration from 0 to 80 phr resulted in an increase in the ML, MH, and delta torque (ΔM) of SBR composites, as well as an increase in t_{s2} and t_{90}. At the same time, increasing the CB content from 20 phr to 80 phr resulted in an increase in the ML, MH, and ΔM. This caused a slight decrease in t_{s2} and t_{90} and therefore an increase in the cure rate. At the same time, the viscosity of SBR composites increased with the addition of CB. Abdelsalam et al. [10] investigated the effect of carbon black (CB) filler loading on mechanical and rheological properties of natural rubber (NR)/styrene-butadiene rubber (SBR)/nitrile butadiene rubber (NBR) ternary rubber nanocomposites. ML, MH, tensile strength, tensile modulus, tear strength, compression set, compression stress, and crosslink density were increased, while the t_{s2}, t_{90}, cure rate index, elongation at break %, swelling coefficient, and filler–rubber interaction decreased with increasing CB loading. Tan and Isayev [11] investigated the effect of silica, CB and nanoclay on the rheological properties and cure characteristics and mechanical properties of EPDM vulcanizates. They reported that silica-filled EPDM compounds exhibited significantly higher storage modulus, loss modulus, and complex viscosity compared with those filled with carbon black. The optimum cure time of silica- and nanoclay-filled EPDM mixtures increased whereas the values for CB-filled EPDM slightly decreased with filler loading. Increasing filler content enhanced hardness, modulus, tensile strength, and elongation at break for all the vulcanizates. The tensile strength and elongation at break of 23.5 MPa and 1045 % was achieved for 30 phr silica filled EPDM vulcanizates, respectively. Bartosik et al. [12] studied the effects of silicon carbide (SiC) and SiC hybrid systems with different conventional fillers (silica, carbon black, graphene, hydrotalcite, halloysite) on the rheometric measurements, crosslink density, mechanical performance, aging stability, morphology, thermal behaviour, and flammability of ethylene-propylene-diene (EPDM) rubber composites. As a result of study, tensile strength increased in the systems with carbon black, silica, and graphene nanoplatelets, by 21 %, 37 %, and 68 %, respectively, compared to the neat EPDM. However, their high costs and the significant energy requirements involved in their production pose limitations to their widespread use. As an alternative, the reinforcement of rubber materials with fibers such as glass, carbon, and aramid — which possess relatively higher elastic modulus — has gained attention for improving the mechanical and thermal properties of rubber composites, offering a viable substitute to traditional fillers like carbon black and silica [9,13–15]. Among various reinforcing fibers, glass fiber is characterized by its low cost, chemical resistance, high strength, excellent insulation properties, good wear resistance, and low creep behavior. Moreover, glass fiber is widely utilized as a primary filler to enhance flame retardancy and improve thermal performance. Its low density also contributes to the reduction of the overall weight of composites in which it is incorporated [16–18]. Taherzadeh-Fard et al. [19] reported that the addition of chopped glass, carbon, and kevlar fibers into a natural rubber matrix altered its mechanical and energy absorption behavior, where kevlar improved ultimate strength, carbon fiber at 5 wt. % optimized deflection-to-failure, and overall fiber addition reduced energy absorption compared to neat natural rubber. Zhang et al. [20] found that incorporating carbon fibers into natural rubber led to uniform fiber dispersion, notable increases in tensile strength (up to 20.9 MPa at 2 wt. %), improved aging resistance, enhanced thermal stability, and more efficient heat conduction compared to the unreinforced natural rubber. Vahidifar et al. [21] investigated the mechanical properties of rubber composites reinforced with nylon fibers and reported that the addition of 10 % fiber reduced the deformation rate while increasing the elastic modulus and the overall service life of the composite. Manchado and Arroyo [22] examined the effects of aramid, glass, and cellulose fibers on the mechanical properties and crosslink density of natural rubber (NR), EPDM, and styrene-butadiene rubber (SBR). Their findings indicated that among the tested fibers, aramid fiber was the most effective in enhancing tensile modulus, strength, and abrasion resistance. Regardless of the rubber type, the incorporation of fibers tended to accelerate the vulcanization rate and increase the crosslink density, particularly in the presence of aramid fibers. Imiela et al. [23] investigated ceramic-forming silicone composites reinforced with different carbon fiber loadings and reported that the incorporation of fibers consistently enhanced the mechanical performance of the rubber composites, with the improvements observed to be independent of the applied specific heat treatment conditions.

In this study, EPDM-based sealing profiles reinforced with glass fiber at loadings of 11, 22, 54, 90, and 145 phr were developed and processed into final products with the aim of preventing damage occurring in sealing elements used for connecting wastewater pipes and during their underground applications, where they are subjected to mechanical forces.

2. Experimental

2.1. Materials

Ethylene Propylene Diene Monomer rubber (EPDM), comprising 48 wt. % ethylene and 5.5 wt. % 5-ethylidene-2-norbornene (ENB), was obtained with grade Keltan 8550 from Arlanxeo. Zinc oxide (Brüggemann, Germany), paraffinic process oil (SK-3, from Petrol Ofisi, Türkiye), stearic acid (Palmata, Indonesia), tetramethyl thiuram disulfide (TMTD) (Vibiplast, Italy), benzothiazole disulfide (MBTS) (Vibiplast, Italy), and sulfur (Berkim, Türkiye) were other ingredients utilized to make the compounds.

2.2. Preparation of compounds

The formulations of the prepared at the phr (per hundred rubber) ratios rubber composites are shown Table 1. EPDM/CE composites were prepared in three stages. Firstly, zinc oxide and stearic acid activators were added to EPDM rubber, and mastication was applied for 35–40 s to bring it to the appropriate viscosity at 35 rpm rotor speed. Then, filler and additive elements such as oil, carbon black and white filler (calcium carbonate, $CaCO_3$) were gradually added and mixed for another 40 s. In the second stage, glass fiber with different rates (11, 22, 54, 90 and 145phr) was added to EPDM rubber and stirred until the temperature reached 100–105 °C. In the last stage, curing agents such as sulphur, MBTS, and TMTD were added to the compound and were stirred for an additional 40 s, or until it reached a temperature of 110–115 °C. The curing characteristics of EPDM/CE including ML, MH, ΔM, cure rate index (CRI), t_{90}, and t_{S2} were determined by TS ISO 6502 at a temperature of 200 °C by using a moving die rheometer (MDR) (Alpha Technologies MDR2000, Set Inc., Turkey). Then, to prepare 2-mm, 6-mm and 12-mm thickness sheets EPDM/CE composites were cured for 40 min at 180 °C using a hydraulic hot press. The Mooney viscosity of both EPDM and EPDM/CE composites was determined with Mooney-viscometer (Alpha MV 2000) following the (1 + 4) criteria at 100 °C, in

Table 1
Formulations of EPDM and EPDM/CE composites.

Component	Parts per hundred rubber (phr)					
	EPDM	11CE	22CE	54CE	90CE	145CE
EPDM	100	100	100	100	100	100
Carbon black	50	50	50	50	50	50
White filler ($CaCO_3$)	20	20	20	20	20	20
Oil	40	40	40	40	40	40
Zinc Oxide	4	4	4	4	4	4
Stearic Acid	2	2	2	2	2	2
Sulfur	1	1	1	1	1	1
MBT	0.5	0.5	0.5	0.5	0.5	0.5
TMTD	1	1	1	1	1	1
Glass fiber (CE)	0	11	22	54	90	145

accordance with ISO 289–1.

2.3. Determination of mechanical and physical properties

The tensile properties of the EPDM/CE composites were evaluated by DIN 53,504 using a universal tensile machine (Zwick-Z020) at a cross-head speed of 200 mm/min using dumbbell-shaped samples. All tests were repeated on five samples from the same composites and average values are reported. After obtaining stress–strain curves, the tensile strength (TS), percentage of elongation at break (% EB), and tensile modulus (at stress at 100 % and 200 % elongations; M100 and M200) values were calculated. The tear strength of B-type samples with 0.5 mm notches was carried out as per ASTM D 624 standard. Compression set tests were conducted using Elastocon-EV 01B following the ISO 815–1 (DIN 53,517) standard, subjecting the specimens to 25 % compression at 100 ºC for 22 h. Abrasive wear tests of EPDM and EPDM/CE composites were carried out using Zwick Roell-6103 according to DIN ISO 4649 (DIN 53,516) standard using a 10 N load and a 200 mm sliding path. The rebound Resilience of EPDM and EDPM/CE composites was measured using the RBN-01 brand Zwick Roell 5109 test device in compliance with the DIN 53,512 standard. Dispersion testing was performed to determine the distribution of carbon black and other filler particles within EPDM rubbers. Dispersion quality measurements, graded from 1 to 10 based on the quantity and size of agglomerations, were conducted in accordance with the ISO 11,345 standard. The hardness of the EPDM and EPDM/CE composites was determined based on ISO 48–4 by the use of a Shore A Type Durometer (SHA-M-01, Bareiss Prüf Gerate). Five measures of Shore A hardness were made at room temperature, and the average was calculated. The fractured surfaces of EPDM and EPDM/CE composites were coated with gold (Baltec SCD005 Sputter Coater-30 mA) and examined with a Quanta 650 Field Emission scanning electron microscope. Using Shimadzu TG-50 equipment, the thermogravimetric analysis (TGA) technique in accordance with TS EN ISO 11,358 was used to assess the thermal behaviour of the samples (Japan). Helium gas was used as the inert atmosphere for the measurements. Samples were placed in ceramic pans and heated at a rate of 10 ºC from room temperature to 1200 ºC. Differential scanning calorimetry (DSC) measurements were conducted on a DSC 3 Mettler Toledo instrument in nitrogen atmosphere at a flow rate of 40 mL/min at heating rates of 10 ºC/min. The glass transition temperature (T_g), decomposition temperature (T_b) and melting heat of fusion (ΔH_m) were estimated from DSC curves.

2.4. Temperature scanning stress relaxation analyses

Temperature scanning stress relaxation (TSSR) measurements were performed using a TSSR instrument obtained from Brabender (Germany) using dumbbell-shaped samples, as defined in ASTM G154–05, and applying the conventional two-step TSSR test method procedure. In the first step, 50 % strain was applied to a dumbbell test specimen (Type 5 A, ISO 527). After the extension was applied, the samples was pre-conditioned for isothermal relaxation at 23 °C for 2 h without heating. As the second step, the sample was heated at a rate of 2 °C/min up to 300 °C. During the stress relaxation process, stress applied to keep the constant strain was monitored and reported versus time and temperature [24–25].

3. Experimental results

The cure characteristic such as ML [26] representing the minimum viscosity of the rubber, and MH [27] representing the crosslinking behavior of the rubber, t_{90}, t_{s2}, and Mooney viscosity of the EPDM/CE composites were determined as a function of the glass fibers content, and the results are given in Table 2. It was observed that ML and MH values increased with increasing CE content in EPDM/CE composites. The values of ML and MH increased by 116.6 % and 79.6 % with the increase of the CE ratio, respectively. It is well known that the increase in torque is due to the higher surface area, greater rubber-filler interactions and consequently, higher retardation in the mobility of rubber chains in the matrix, resulting in higher compound viscosity and crosslink density [28–30]. A similar result was reported by Wen et al. [31] and the torque values significantly increased with the addition of aramid fiber (AF) in the AF/EPDM composite. Table 2 also shows the effects of CE content on the t_{S2} and t_{90} of EPDM/CE composites. For EPDM and EPDM/CE composites, a noticeable decrease in t_{S2} and t_{90} is observed with the addition of the CE, which seems to indicate that the CE used in this study accelerate the vulcanization reaction of the EPDM rubber. A similar result was obtained in the study by Meissner [29] and Lopez Manchado [22]. ΔM value calculated from the difference between ML and MH is closely related to the crosslink density of the mixture [32]. The ΔM value of EPDM rubber reached 19.41 dNm from 10.99 dNm for 40CE composite. Therefore, the higher ΔM value suggests that the 145CE composite may possess the highest crosslink density, which is also supported by the experimentally determined crosslink density values will be seen later in Table 4. Additionally, the t_{s2} and t_{90} values indicate that the 145CE composite began to cure much earlier and had a shorter optimum curing time. Another important rheological parameter characterizing the curing of rubber compounds is the cure rate index (CRI). The CRI increased from 105.26 to 117.64 with increasing CE content from 0 to 145 phr in the EPDM/CE composites, as shown Table 2. Maged et al. [33] reported that CRI values was increased with $CaCO_3$ addition and depended mainly on the concentration and the type of the rubber. The addition of CE did not affect the Mooney viscosity of the EPDM/CE composites. The Mooney viscosity of the EPDM rubber was as 64.1 MU, whereas the corresponding values for the 11CE, 22CE, 54CE, 90CE, and 145CE composites were as 63.2, 63.8, 63.1, 61.8, and 62.1 MU, respectively. The hardness values of the rubber vulcanizates mainly depend on the type of rubber, the amount of filler and the cross-link density. In most cases, high level of cross-link density causes rubber vulcanizates to have relatively higher hardness values [34]. Table 2 also shows the effect of CE content on the Shore A Hardness (ShA) of EPDM and EPDM/CE composites. The result showed that there is a steady increase in ShA of EPDM/CE composites with an increase in CE content. EPDM rubber has a 56 ShA; as CE were added, the ShA increased to 61, 64, 71, 76 and 85 for 11CE, 22CE, 54CE, 90CE and 145CE, respectively. It is expected because as filler particles are added to rubber matrix, there is a corresponding reduction in the elasticity (fibers fill the spaces between rubber chains) of the rubber thereby resulting in more rigid rubber vulcanizates [22,34]. Shamsabadi et al. [35] stated that the hardness of EPDM, which was 51 ShA, was increased to 72 ShA with the addition of 60 phr CB, and that this could be due to the physical interactions between the EPDM chains and the CB active surfaces and the segmental mobility of the EPDM chains. Manjhi et al. [36] observed a similar improvement in the ShA as a function of filler loading in to the EPDM rubber. The higher the degree of crosslinking by means of either sulfur or peroxide vulcanization, the greater tendency of physical crosslinking, empowering the EPDM to resist the deformation. Higher crosslink density in EPDM composites determines higher values of ShA

Table 2
Effect of CE filler content on the cure characteristics and Mooney viscosity of EPDM/CE composites.

	EPDM	11CE	22CE	54CE	90CE	145CE
ML (dNm)	0,90	0.97	1.08	1.15	1.47	1.95
MH (dNm)	11.89	12.65	13.71	14.59	17.55	21.36
Delta torque (ΔM) (dNm)	10.99	11.68	12.63	13.44	16.08	19.41
t_{s2} (min)	0.45	0.44	0.41	0.40	0.41	0.38
t_{90} (min)	1.40	1.35	1.28	1.27	1.25	1.23
CRI	105.26	109.89	114.94	114.94	119.04	117.64
ML (MU)	64.1	63.2	63.8	63.1	61.8	62.1
Hardness, Shore A	56	61	64	71	76	85

(Tables 2) [37].

The strength of fibre filled rubber composites depends on the strength of the rubber matrix, rubber–fibre interaction, the degree of wetting of fibre particles by the rubber macromolecular chain [38]. The effect of CE content on the stress-strain plots of EPDM/CE composites was shown in Fig. 1. At low strains (below 50 %), the initial slope of stress-strain curves took on a sharp increase with the increase of CE content. The stress-strain curves of EPDM composites with low CE loadings (11 and 22 phr) were similar to those of EPDM rubber and did not show obvious yield phenomenon. The stress-strain curves showed a pronounced yield point at high CE loadings, and the yield strain value was shifted toward low strain direction owing to the uneven dispersion of CE in the EPDM/CE composites. For fiber filled rubber composites, the yield phenomenon meant that the interfacial debonding occurred between CE and the matrix as a result of applied shear stress. The weak interaction between the CE and the EPDM rubber leads to failure of the interface, which appears as necking in the stress-strain curves. After the yield point, the reinforcing effect of CE would basically disappear with further deformation. At high CE loadings, the stress-strain behavior of EPDM/CE composites would be gradually dominated by the interfacial interaction between CE and EPDM rubber, resulting in the decrease of EB and tensile strength [39].

Fig. 2 illustrates SEM morphologies of the tensile fracture of both EPDM and EPDM/CE composites. The effect of CE addition on EPDM composites, as well as the behavior of the fiber-matrix interface and pullout effects, were evaluated using SEM images. The fracture surface of EPDM (Fig. 2 a) appears relatively smoother compared to 11CE, 22CE, 54CE, 90CE and 145CE. As shown in Fig. 2 b–d, it is evident that 11, 22 and 54 phr of CE is uniformly dispersed in the EPDM rubber, displaying homogenetiy, with no noticeable critical agglomeration of the CE. This was confirmed by the results of mechanical tests because these material showed highest tensile strength because of the CE might be better dispersion in the EPDM rubber to have provided sufficient filler-matrix stress transfer for improved mechanical properties. In contrast, as seen in Fig. 2 e-f, the number of CE and fiber–fiber contact increases with the increasing amount of CE. The addition of 90 and 145 phr of CE into EPDM rubber resulted in a more irregular texture and increased surface roughness, with increased agglomeration of CE, at the fracture surface of EPDM/CE composites. It was also observed that both the pullout mechanism and the fiber breakage mechanism were dominant in the EPDM composites containing 90 phr and 145 phr CE. In addition, some gaps between CE and EPDM rubber can also be found on the fracture surface, indicating that the CE–EPDM interface is not so strong, which results in debonding. This was confirmed by the results of strength tests because these materials showed low tensile strength. Similar results are obtained by Sau et al. [38].

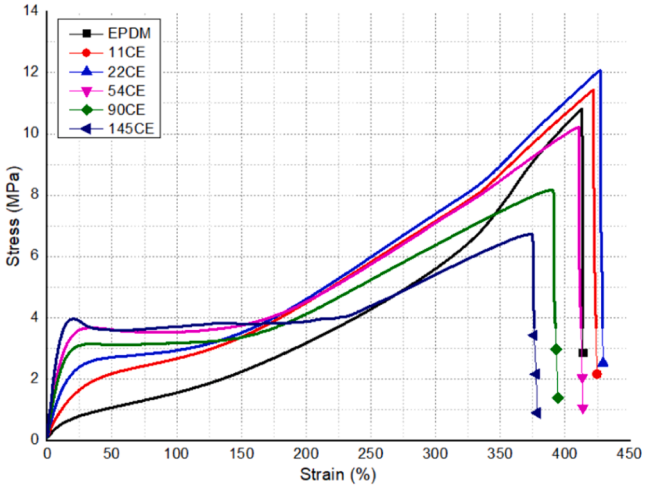

Fig. 1. Stress-strain curves of EPDM and EPDM/CE composites.

Fig. 3 show the effect of CE content on the tensile modulus (M100 and M300) of EPDM and EPDM/CE composites. It can be seen that M100 and M300 increase with increasing CE content. The M100 of the 145CE composite increased by 127.7 %, reaching 4.1 MPa, compared to EPDM rubber. Meanwhile, the M300 of the 145CE composite increased by 19.7 %, reaching 8.5 MPa. The increase in tensile modulus is also reported by Yeşil and Karaagac [40] and by El Mogy et al. [27]. The enhancement of the modulus in EPDM/filler composites is attributed to fiber shape and high modulus of CE and the strong interactions between filler and EPDM, which improve the stiffness and therefore reduce the deformability under applied stress, as previously noted by Abdelsalam et al. [10] and Wang et al. [39]. The strong interactions between rubber and filler reduce elasticity (enhanced the stiffness) and restrict the movement of rubber chains, leading to EPDM rubbers that are tough and more rigid [27,41–42].

Fig. 4 shows the effect of CE content on the tensile properties of the EPDM/CE composites. According to Fig. 4 (a), when the content of CE increases to 22 phr, the tensile strength of the EPDM/CE composites increases to 12.1 MPa, which is improved by 9 % compared with that of the EPDM rubber. This is because the uniform dispersion of CE in the EPDM rubber endows better adhesion between CE and the EPDM rubber [43]. When the reinforced fiber composite is subjected to load, the fibers act as carriers of load and stress is transferred from matrix along the fibers leading to effective and uniform stress distribution [29]. However, the tensile strength of EPDM/CE composites started to decrease with 54 phr content. Agglomeration or clustering of CE particles (Fig. 2 e and f) occurred at high filler content (90 phr and 145 phr CE) and caused weak areas in the EPDM/CE composite. Abdelsalam et al. [10] also reported that agglomeration occurs above 45 phr CB, and therefore, particle–particle interaction of the CB is responsible for the observed decrease in tensile strength. They stated that the formation of CB aggregates led to the formation of weak points in the ternary rubber phase and decreased the tensile property (5.28 MPa). The decrease in tensile strength may also result from the different surface characteristics of the fiber and the matrix. The hydrophilic and polar nature of the fiber, in contrast to the hydrophobic and non-polar nature of the polymer matrix, reduces fiber–matrix compatibility and interfacial adhesion [44]. In polymer technology, one of the most common approaches to improve interfacial bonding is the surface modification of fibers using silane coupling agents [44–45]. Hayichelaeh et al. [46] reported that incorporating silane-modified fillers into natural rubber enhanced filler–elastomer interactions, reduced filler–filler interactions, and lowered rubber viscosity, which is advantageous for both processing and vulcanizate properties. Arslan and Doğan [47] demonstrated that the use of a silane coupling agent increased tensile strength, flexural strength, and elastic modulus. Jacob et al. [48] stated that alkali-treated fibers improved the tensile properties compared to untreated composites because they increased the degree of adhesion between the fiber and the matrix. The CE filler was not able to properly transfer the stresses from the rubber matrix, resulting in low tensile strength in the 54CE, 90CE and 145CE composites. The tensile strength of these composites decreased by 7.2 %, 26.0 %, and 39.5 % compared to the neat EPDM rubber, respectively. This behaviour is in agreement with the study carried out by Sobhy and Tammam [28], Zhang et al. [20], Asghar et al. [49].

As seen in Fig. 4 (b), the elongation at break increased up to 22 phr CE content, after this value it decreased with increasing CE content. At a CE filler content of 22 phr, the elongation at break is improved from 412 % (EPDM rubber) to 426 % in average, which is an increase of 3.4 %. Increase in the elongation at break values can be attributed to lower initial tensile modulus values (Fig. 2), which are also in a good correlation with lower cure torque increment for EPDM rubber [50]. After 22 phr CE content, the elongation at break decreased by 8.9 % at 145 phr CE filled EPDM composites, compared to the EPDM rubber. The elasticity can dramatically decrease because of the formation the network of

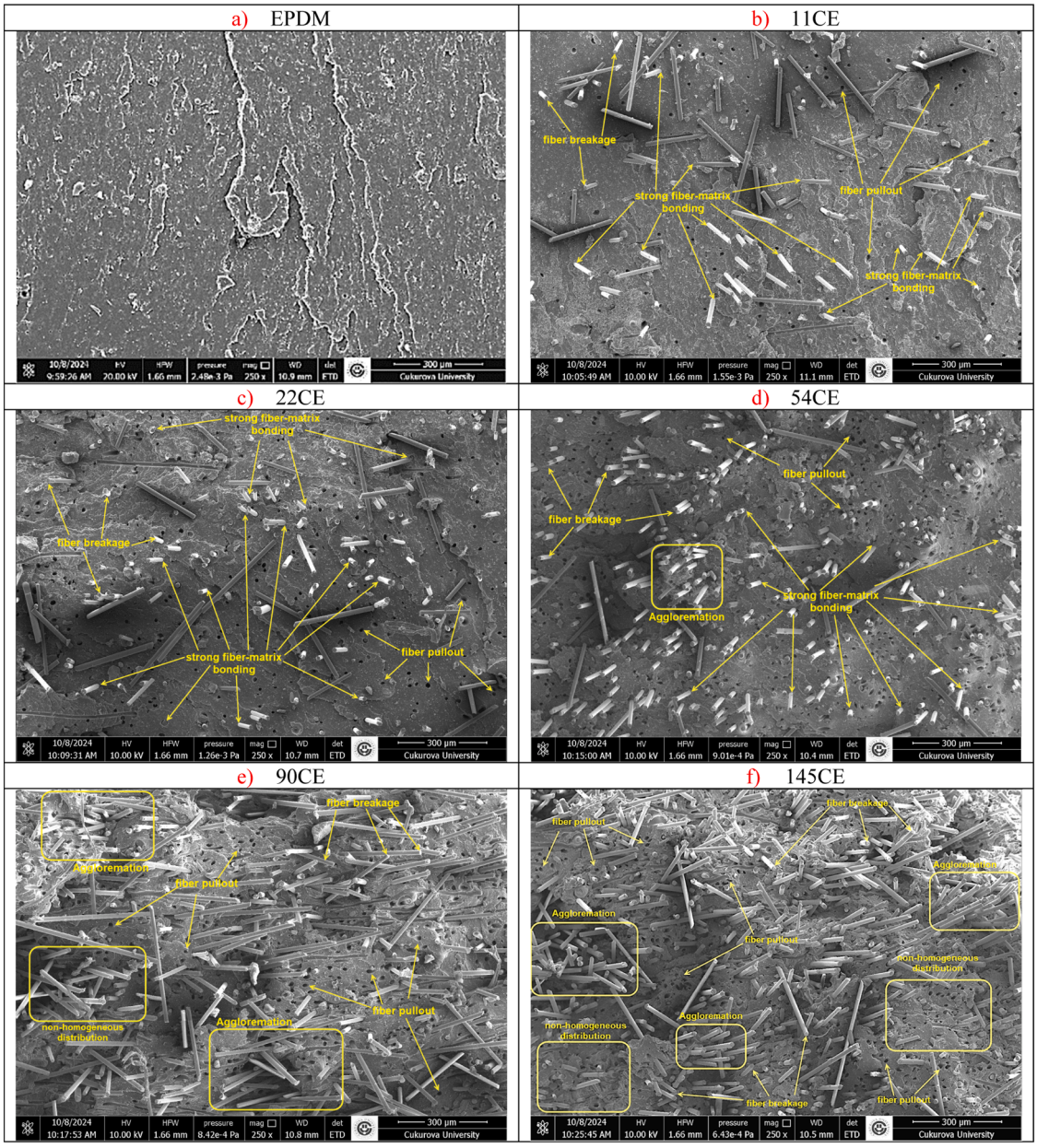

Fig. 2. SEM images of fracture surface of EPDM and EPDM/CE composites.

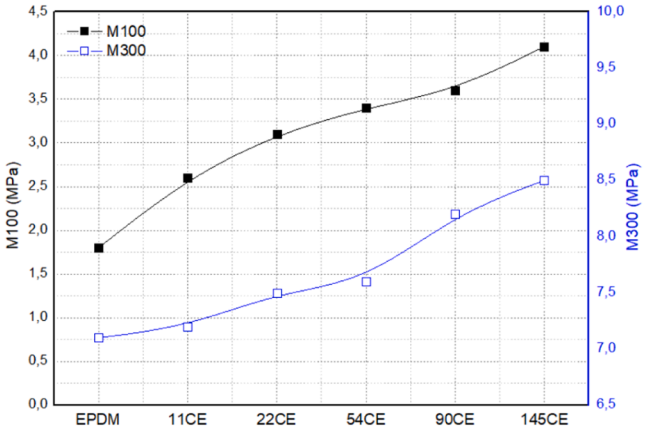

Fig. 3. Tensile modulus of EPDM and EPDM/CE composites.

CE in EPDM rubber, which restrains the movement of chain segments in the rubber chains [28]. Khalaf [9] reported that the addition of silica increases the TS and M100 up to 60 phr, while the elongation at the break increases up to 40 phr silica and then undergoes an abrupt decrease on further loading. Whereas, a dramatic increase in TS and M100 was observed at nearly all levels of the CB filled SBR rubber due to increasing polymer–filler interactions and filler–filler interactions, which restrict the mobility of the soft SBR phase. Furthermore, the ductility of rigid fiber is worse than that of the polymer matrix, which indicates that the fiber hinders the deformation of the polymer matrix before it breaks [51]. Increased fiber loading in the rubber matrix resulted in the composite becoming stiffer and harder. This will reduce the composite's resilience and toughness and lead to lower elongation at break [29,52].

Tear strength and compression set changes depending on the CE content of EPDM and EPDM/CE composites are given in Fig. 5. Tear strength indicates the durability and toughness of rubber. Longer service life is associated with higher tear strength, which is an indicator of

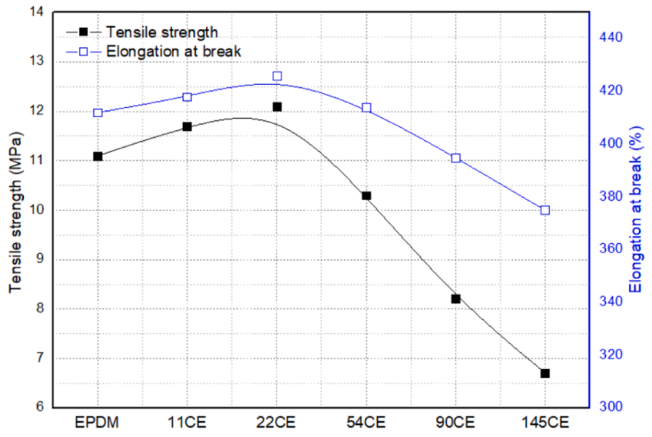

Fig. 4. a). Tensile strength, b) Elongation at break of EPDM and EPDM/CE composites.

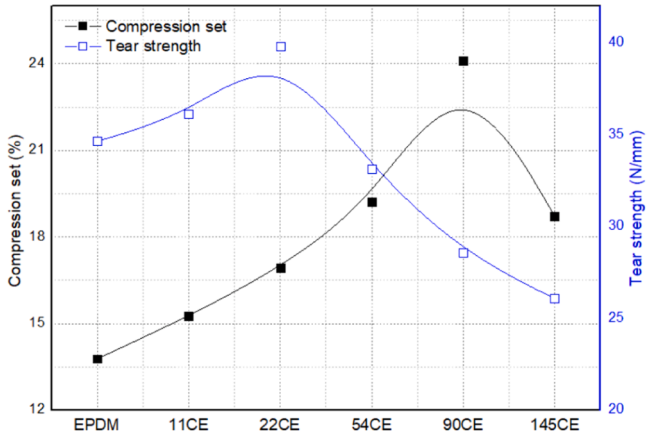

Fig. 5. a). Compression set and b) tear strength of EPDM and EPDM/CE composites.

resistance to fracture propagation [53]. As seen in Fig. 5, at high fiber loadings, tear strength is found to decrease as the increased between fibers strain in the matrix increases tearing therefore reduces the tear strength. Tear strength reduced with the addition of 145 phr of CE by 35.9 %, compared to EPDM rubber. The non-uniform distribution of fillers in EPDM rubber and bigger agglomerates of filler in EPDM rubber (see Fig. 2 f) may be responsible for the decreased tear resistance by reducing crack growth resistance [10]. According to these results, it can be clearly assumed that the fibers behave as effective reinforcing agents for rubber compounds, especially at the lower fiber content. Compression set measures the ability of rubber to return to its original thickness after prolonged compression at a given deflection [54]. A low compression set value indicates the sample's ability to maintain its original thickness while having low damping capabilities, while a large compression set indicates lower stiffness but higher damping properties [10]. Fig. 5 presents the compression set values as a function of the CE content. The compression set values for the EPDM, 11CE, 22CE, 54CE, 90CE and 145CE composites are found to be 13.78, 15.25, 16.93, 19.22, 24.12 and 18,73 %, respectively. The compression set performance of EPDM/CE composites increased markedly with CE loading up to 90 phr, but exhibited a decline at 145 phr CE. The increase in compression set values with increased fiber loading results from the stiff nature of the fibers and increasing crosslinking density of the EPDM/CE composites. This restricts the mobility of the rubber chains resulting in decrease of elastic deformation and recovery of the EPDM matrix [55–56]. The change in compression set value is also likely due to microstructural changes such as fiber agglomeration, void formation, and weak interfacial interaction. Agglomeration disrupts the homogeneous distribution of fibers, increasing fiber-to-fiber interaction in some areas, which can further complicate elastic recovery dynamics and permanent deformation. Shen et al. [57] indicated that homogeneous distribution of fibers leads to low compression set, while the breakdown of large agglomerates in rubber under compression stress causes the high compression set. The best material was obtained as the 11CE composite with the lowest compression set value.

Fig. 6 shows the change in wear loss and rebound resilience of EPDM and EPDM/CE composites depending on CE content. Rebound resilience values ranged from 63 % to 47 % for EPDM and EPDM/CE composites. The EPDM/40CE composite exhibited a 25.1 % lower rebound resilience than EPDM rubber. The rebound resilience of EPDM/CE composites decreased with increasing CE content. This is due to the restriction of molecular mobility caused by increasing filler concentration, hardness, and crosslink density [37,58]. As was previously mentioned, the incorporation of the fibers gives rise to a more rigid material, with a significant decrease of the elastic properties of the elastomer. In fact, the addition of the fibers produces a marked decrease of the rebound resilience and an increment of the compression set [22]. The tribological properties of rubbers is affected by the chain flexibility of the main matrix, as well as the type and amount of filler, and the interaction between the rubber and the filler [50,59]. Wear loss values for EPDM and CE filled EPDM composites are give in Fig. 6. It is seen from the figure that wear loss decreases accordingly as the CE content increases. The lowest wear loss was obtained in the 145 phr CE filled EPDM composite. The decrease in wear loss with increasing CE content for EPDM/CE composites is evidence of the fillers' potentials to withstand or hinder the progressive removal of materials from the surface of the EPDM/CE composites. The highest abrasion resistance (the lowest wear loss) corresponds to its highest hardness and crosslink density, which is related to the highest torque difference (Tables 2). Fig. 7 also shows the relationship between specific wear rate (SWR) and ShA. As seen in Fig. 6, SWR decreased dramatically as ShA values increased. The reduction in SWR of EPDM/CE composites may be due to the homogeneous distribution of the CE filler, which may have led to a good matrix–reinforcement interaction. These results are in agreement with [60].

The thermal properties of EPDM and EPDM/CE composites was analyzed using differential scanning calorimetry (DSC), and the DSC thermograms and thermal transition parameters are given Fig. 8 and Table 3, respectively. According to the results, the glass transition temperature (T_g) of EPDM rubber was -33.51 °C, and the T_g of EPDM/CE composites exhibited ranging between −34.35 °C (11CE) and −29.34 °C (145CE) with increasing CE. The addition of CE restricted the molecular

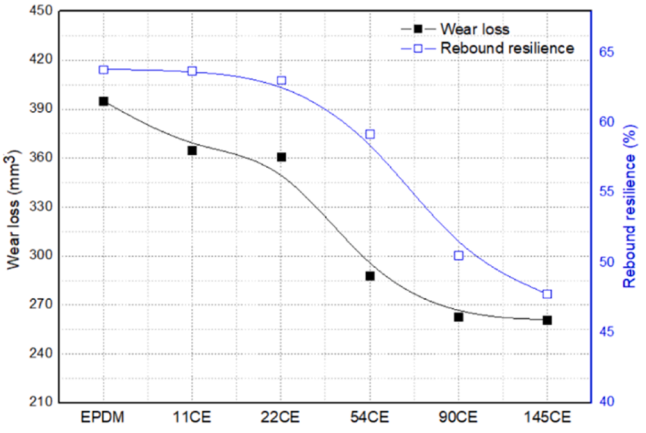

Fig. 6. a). Wear loss, and b) rebound resilience of EPDM and EPDM/CE composites.

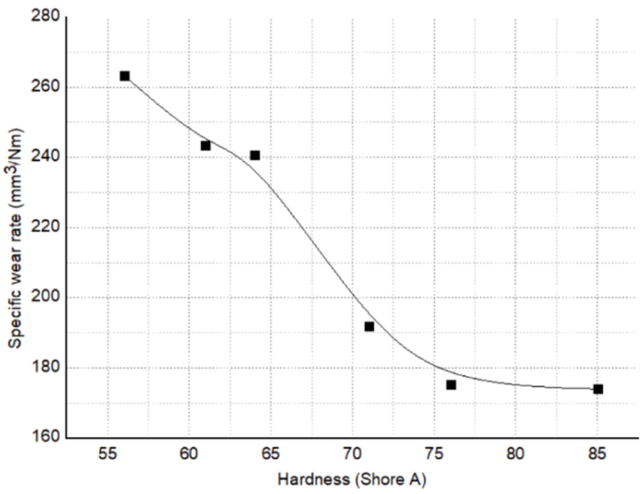

Fig. 7. The relationship of SWR and ShA of EPDM and EPDM/CE composites.

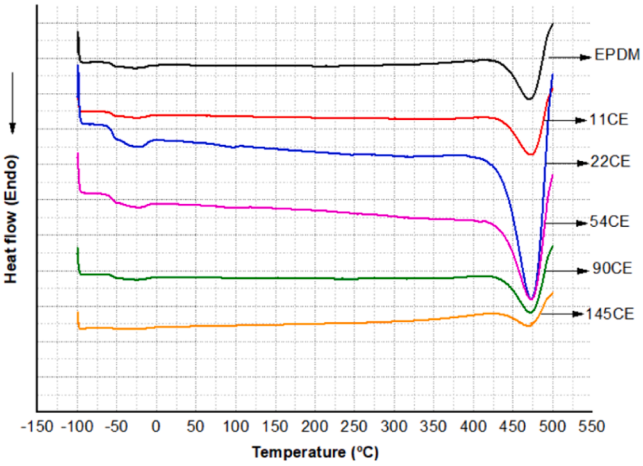

Fig. 8. Melting (endothermic) thermograms of EPDM and EPDM/CE composites.

Table 3
Melting values of samples according to endothermic DSC results.

	Glass transition temperature, T_g	Decomposition temperature, T_b	ΔH_g, (J/g)	ΔH_b, (J/g)
EPDM	-33.51	468.84	10.66	97.47
11CE	-34.35	473.59	11.52	99.94
22CE	-32.21	472.02	10.40	110.21
54CE	-33.70	472.64	10.11	95.18
90CE	-31.36	471.43	9.12	75.57
145CE	-29.34	469.49	9.22	40.56

mobility of the EPDM rubber due to enhanced filler–matrix interactions and shifted the T_g value to higher values. This is consistent with previous studies that found a slight increase in T_g with the addition of silica to the polymer matrix [61]. The decomposition temperatures (T_b) of the EPDM/CE composites remained relatively stable, with values between 468.84 °C and 473.59 °C, indicating that CE addition did not significantly compromise the thermal stability of EPDM rubber. Endothermic enthalpy changes (ΔH_g and ΔH_b) exhibited a more pronounced variation. While ΔH_g values ranged from 9.12 to 11.52 J/g, ΔH_b showed a drastic reduction from 97.47 J/g in EPDM to 40.56 J/g at 145CE.

The decomposition temperatures and thermal stabilities of EPDM and EPDM/CE composites were determined using TGA analysis, and the resulting thermograms are shown in Fig. 9. It was determined that the

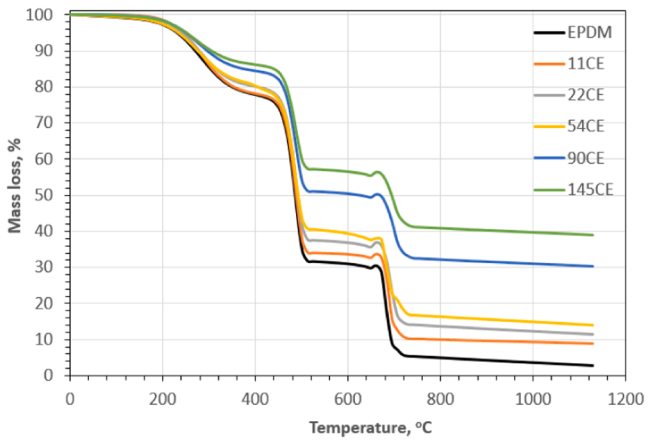

Fig. 9. Thermogram of TGA of EPDM and EPDM/CE composites.

thermal degradation process proceeds through four distinct temperature regions: (i) 0–250 °C, (ii) 250–450 °C, (iii) 450–650 °C, and (iv) above 650 °C. The small weight loss in the first stage corresponds to the removal of oil from the compound. The weight loss in the second stage occurs at temperatures above 450 °C and is due to the decomposition of the EPDM chains. However, at approximately 650 °C, calcium carbonate begins to break down into calcium oxide and lose weight. The temperature rise from 485.9 ℃ (EPDM rubber) to 694.4 ℃ (145CE composites) when the weight loss is 50 %, which prove that heat can be transferred to the matrix through the CE quickly when the rubber composites is heated gradually. As shown in the figure, stability of the structure was achieved at temperatures higher than 700 ℃. The decomposition temperature of the EPDM/CE composites increased with increasing CE content. While the decomposition temperature of EPDM rubber was 718 ℃, the decomposition temperatures for 11CE, 22CE, 54CE, 90CE, and 145CE composites were 718, 729, 729, 738, and 741 ℃, respectively. The heat inside the rubber composites is uniform because of homogenous distribution and the good interaction between filler and rubber, therefore, the weight loss of the fiber filled rubber composite slowed down and the decomposition temperature occurred at higher temperatures [20,49,62].

Isothermal relaxation test results for EPDM and EPDM/CE composites at ambient temperature after 50 % strain are given in Fig. 10. Absolute isothermal relaxation is given in Fig. 10-a, and the normalized stress-time relaxation curve is given in Fig. 10–b. As can be seen from the figures, the relaxation rate of EPDM rubber is higher than that of EPDM/CE composites. The non-isothermal temperature-scanning relaxation behavior of EPDM and EPDM/CE composites is shown in Fig. 11. Evaluating the relaxation curves, it was observed that EPDM rubber has a T_{90} temperature of 300 °C. The T_{90} temperature decreased with the addition of different amounts of CE to the EPDM rubber. The parameters obtained from the non-isothermal relaxation curves of EPDM and CE-filled EPDM composites in TSSR tests are given in Table 4. The T10, T50, and T90 values represent the temperatures at which the initial strength decreases by 10 %, 50 %, and 90 %, respectively, during the non-isothermal temperature-scanning stress relaxation process. The addition of CE to EPDM rubber reduced the T10, T50, and T90 temperatures. The initial stress (σo) of glass fiber-reinforced EPDM rubber under non-isothermal conditions (stress after 2 h of isothermal relaxation at 50 % strain) increased by 181.6 % from 0.60 MPa to 1.69 MPa. The increase in stress values with the addition of CE to EPDM rubber can be attributed to the strength-enhancing properties of the glass fiber additive. The interaction between the polymer and the additive increases with the increase in the glass fiber content, resulting in a harder/stiffer EPDM rubber and higher stress levels. These increases in initial stress values under both isothermal and non-isothermal conditions suggest that stretching is increased due to increased crosslink density. There is a relationship

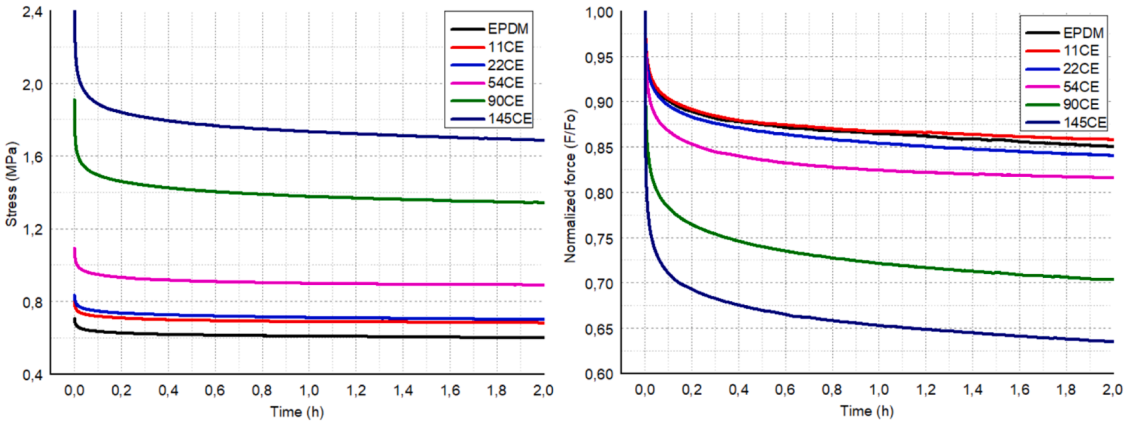

Fig. 10. Isothermal stress relaxation curves of EPDM and EPDM/CE composites (a) Absolute isothermal relaxation curve, (b) Normalized isothermal relaxation.

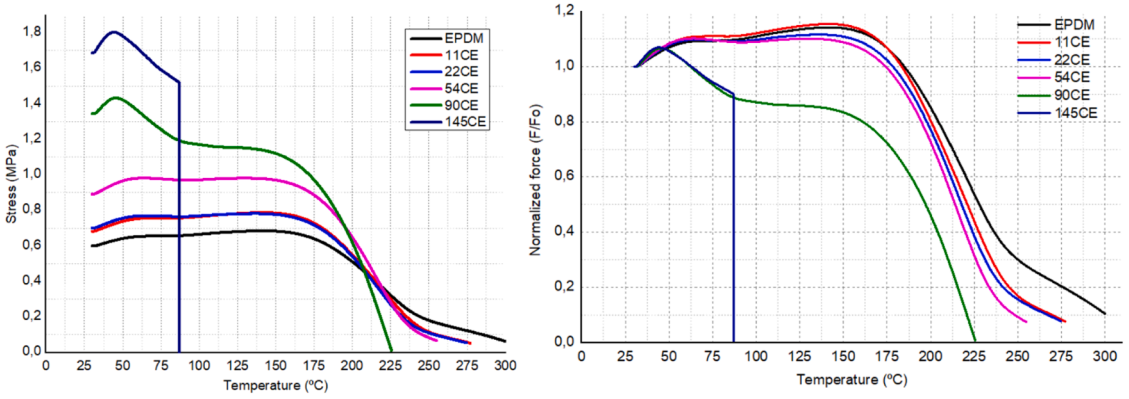

Fig. 11. Anisothermal temperature scanning stress relaxation curves of EPDM and EPDM/CE composites.

Table 4
TSSR parameters obtained from stress-temperature curves of EPDM and EPDM/CE composites.

	EPDM	11CE	22CE	54CE	90CE	145CE
σo (MPa)	0.60	0.68	0.70	0.89	1.34	1.69
T10 (°C)	195.6	192.7	189.5	186.2	83.0	87.0
T50 (°C)	227.9	221.1	217.9	214.1	197.2	87.0
T90 (°C)	300.1	269.6	267.2	248.3	220.8	87.1
Integral (K)	221.7	211.1	204.3	196.5	152.1	56.5
TSSR-Index (RI)	0.82	0.88	0.86	0.90	0.80	0.99
k0 (Pa/K)	1947.8	2447.4	2506.5	3520.0	7298.1	10,319.9
ν (mol/m^3)	221.94	278.86	285.60	401.08	831.56	1175.87

between the anisothermal relaxation initial force (σ0) and the crosslink density. Increasing the crosslink density results in an increase in the σ0 value. The Rubber Index (RI) (TSSR-Index) is a parameter used to characterize the elastomeric behavior of a sample. It is calculated by dividing the area under the stress-temperature curve (A) by the span length (T90-T0). A higher TSSR-Index value indicates more rubber-like behavior, while a lower RI value indicates a possibility of deviation from the elastomeric properties. The RI value of 0.82 for EPDM rubber increased with the addition of CE, and an RI of 0.99 was obtained for 145CE rubber. This is thought to be due to the strong interaction between CE and EPDM rubber. A higher additive-polymer interaction can lead to a higher crosslink density, which in turn can lead to an increase in rubber behavior (more thermomechanically stable). While the crosslink ratio (ν) of EPDM rubber was 221.94 mol/m^3, it increased with the addition of CE and the increasing amount of CE and was obtained as 1175.87 mol/m^3 in the 145CE sample. These results seem to indicate that the CE present a higher adhesion to the EPDM rubber, which improves the efficiency of vulcanization by increasing the degree of organization of the polymer molecules [22].

Table 5 shows the initial stress (σs) at the lowest isothermal conditions was 0.70 MPa for EPDM rubber, while the initial stress increased with increasing glass fiber content, resulting in a stress of 2.66 MPa for the 145CE sample. As the crosslink density increases, the stress required to stretch the material by 50 % also increases, as the rubber chains get closer to each other. Therefore, it becomes more difficult for the applied stress to subside; in other words, the relaxation rate decreases. Since the relaxation behavior of the material decreases as the crosslink density increases, the F(stress)-t(time) curve allows an assessment of the material's crosslink density [63–64].

The dispersion test results of EPDM and EPDM/CE composites are presented in Fig. 12 and Table 6. The dispersion rate of EPDM and EPDM/CE composites was discovered to be between 80 % and 96 %. When Fig. 12 and Table 6 were evaluated, 3.76 %, 7.70 %, 14.19 %, 8.95 %, 12.18 % and 19.50 % white area was determined in 11CE, 22CE, 54CE, 90CE and 145CE, respectively. This amount of white area

Table 5
TSSR parameters obtained from stress-time curves of EPDM and EPDM/CE composites.

	EPDM	11CE	22CE	54CE	90CE	145CE
Fs (N)	6.5	7.1	7.4	8.8	15.6	21.2
Fo (N)	5.5	6.1	6.3	7.2	11.0	13.5
σs (MPa)	0.70	0.79	0.83	1.09	1.91	2.66
σo (MPa)	0.60	0.68	0.70	0.89	1.34	1.69
A (MPa)	0.11	0.11	0.13	0.20	0.57	0.97
α	-2.42	-2.43	-2.46	-2.55	-2.77	-2.88

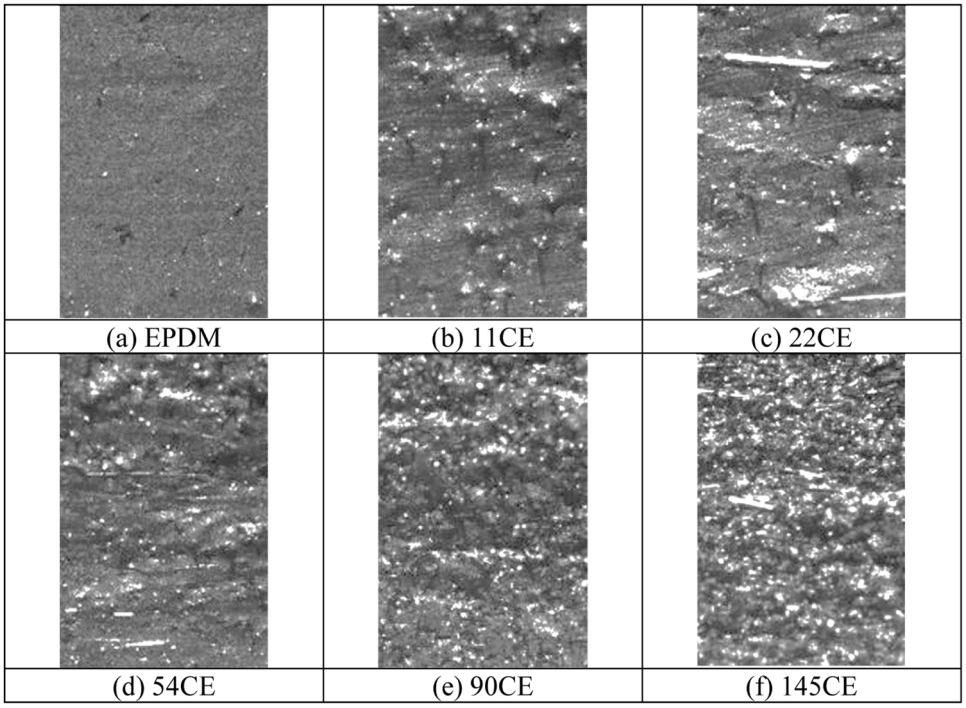

Fig. 12. Dispersion images of EPDM and EPDM/CE composites.

Table 6
Dispersion test results of EPDM and EPDM/CE composites.

	X	Y	Z	White area, %	Dispersion, %	Average Agg. Size, [μm]	Agg. Size Std. Dev [μm]
EPDM	3.38	9.94	89,26	3.76	96,4	2.82	2.42
11CE	1.67	8.03	78.01	7.70	92.3	3.47	5.44
22CE	1.03	6.20	59.45	14.19	85.8	3.59	5.81
54CE	1.42	8.11	74.43	8.95	91.0	3.62	5.18
90CE	1.00	6.46	65.19	12.18	87.8	3.79	6.56
145CE	1.00	3.48	44.29	19.50	80.5	3.68	7.37

provides information about whether white fillers in the rubber are mixed homogeneously with other components. The smaller white area in % and average agglomerate size, more homogeneously distributed white fillers in EPDM rubbers. The "x" and "y" parameters are also used to determine the distribution's quality. The "x" parameter describes the size of the agglomeration, whereas the "y" parameter describes how the agglomeration sizes are distributed. For filled mixtures, $x \geq 2.5$ and $y \geq 5$ means that the fillers in the mixture are distributed homogeneously [40,59]. Accordingly, the distribution index decreased with increasing CE content, indicating a progressively less homogeneous dispersion of CE within the EPDM matrix. Mechanical test results further demonstrated that the incorporation of 54 phr CE represents the optimum loading level, providing superior performance compared with the other CE concentrations.

4. Results

The primary objective of this research was to examine how the addition of glass fiber (CE) filler impacts the curing characteristics, mechanical properties, and thermal behavior of EPDM and EPDM/CE composites. The following results were obtained in the experimental study conducted on EPDM and CE filled EPDM composites.

- Compared to EPDM rubber, the M100 tensile modulus of the 145CE composite increased by 127.7 % to 4.1 MPa, and the M300 tensile modulus increased by 19.7 % to 8.5 MPa.
- Tensile strength values increased up to a 22 phr CE content and then decreased with further increases in CE content.
- The tear strength of EPDM rubber decreased with the addition of CE. The addition of 145 phr CE reduced tear strength by 35.9 % compared to EPDM rubber.
- The highest compression set value, 24.12 %, was observed in EPDM composites with a 54 phr CE addition.
- The rebound resilience values of EPDM and EPDM/CE composites were obtained between 63 % and 47 %. CE fillers reduced the rebound resilience of EPDM/CE composites.
- The T_g value of EPDM rubber was -33.51 °C, and the Tg value increased to -29.34 °C with increasing CE content.
- The decomposition temperature of EPDM rubber was 718 ºC, while 718, 729, 729, 738, and 741 ºC were obtained for 11CE, 22CE, 54CE, 90CE, and 145CE composites, respectively.
- The crosslink ratio (ν) of EPDM rubber was 221.94 mol/m^3, and increased with the addition of glass fiber and the increasing glass fiber content, reaching 1175.87 mol/m^3 in the 145CE sample.
- As a result of the study, EPDM composites with improved thermal properties, improved mechanical and physical properties and wear resistance were produced with the addition of different amounts of glass fiber.

CRediT authorship contribution statement

Gizem Halitoğulları: Validation, Methodology, Investigation. **İlker Köprü:** Validation, Methodology, Investigation, Data curation. **Sinan Köse:** Visualization, Software, Resources, Methodology. **Fatma Ulusal:** Writing – original draft, Software, Methodology, Investigation. **Salih Hakan Yetgin:** Writing – review & editing, Writing – original draft, Project administration, Methodology, Investigation, Data curation, Conceptualization.

Declaration of competing interest

The author is an Editorial Board Member/Editor-in-Chief/Associate Editor/Guest Editor for this journal and was not involved in the editorial review or the decision to publish this article.

The authors declare the following financial interests/personal relationships which may be considered as potential competing interests: Salih Hakan YETGİN reports that financial support was provided by TÜBİTAK Scientist Support Programs Directorate (BIDEB). (Project No: 1139B412304113). If there are other authors, they declare that they have no known competing financial interests or personal relationships that could have appeared to influence the work reported in this paper.

Acknowledgements

This study was supported by the TÜBİTAK Scientist Support Programs Directorate (BIDEB, 2209-B). (Project No: 1139B412304113).

Data availability

Data will be made available on request.

References

[1] P. Rybinski, B. Syrek, A. Marzec, B. Szadkowski, M. Kusmierek, M. Sliwka-Kaszynska, U.Z. Mirkhodjaev, Effects of basalt and carbon fillers on fire hazard, thermal, and mechanical properties of EPDM rubber composites, Materials 14 (18) (2021) 5245, https://doi.org/10.3390/ma14185245.

[2] C. Zhang, J. Wu, F. Teng, B. Su, Y. Wang, H. Ao, Theoretical and experimental characterization for macro-micro friction behaviors of EPDM rubber, Polym. Test. 99 (2021) 107213, https://doi.org/10.1016/j.polymertesting.2021.107213.

[3] A.A. Abdelsalam, W.S. Mohamed, G.A El-Naeem, S.H. El-Sabbagh, Effect of the silane coupling agent on the physicomechanical properties of EPDM/SBR/AL2O3 rubber blend nanocomposites, J. Thermoplast. Compos. Mater. 36 (5) (2022) 1811–1832, https://doi.org/10.1177/08927057211067702.

[4] J. Kruzelak, M. Mikolajova, A. Kvasnicakova, M. Dzuganova, I. Chodak, J. Hronkovic, J. Preťo, I. Hudec, Combined sulfur and peroxide vulcanization of filled and unfilled EPDM based rubber compounds, Mater 16 (16) (2023) 5596, https://doi.org/10.3390/ma16165596.

[5] C. Sung-Seen, K. Yun-Ki, Analysis of 5-ethylidene-2-norbornene in ethylene-propylene-diene terpolymer using pyrolysis-GC/MS, Polym. Test. 30 (2011) 509–514, https://doi.org/10.1016/j.polymertesting.2011.04.005.

[6] B. Rodgers, H. Waddell, R Compunding, Eds.: Cohen P., D'Sidocky M., Encyclopedia of Polymer Science and Technology, 3rd ed., Wiley Blackwell, United Kingdom, 612–670, 2004.

[7] A.T. Bayram, B. Karaagac, H. Konyalı, Evaluatıng ethylene propylene dıene monomer rubber for dynamıc applıcatıons ınstead of natural rubber, Eskişehir Technical Univ, J. Sci. Tech. A – Appl. Sci. Eng. 20 (1) (2019) 121–132, https://doi.org/10.18038/aubtda.410141.

[8] M.D. Frogley, D. Ravich, H.D. Wagner, Mechanical properties of carbon nanoparticle-reinforced elastomers, Compos. Sci. Technol. 63 (11) (2003) 1647–1654, https://doi.org/10.1016/S0266-3538(03)00066-6.

[9] E.S.A. Khalaf, A comparative study for the main properties of silica and carbon black filled bagasse-styrene butadiene rubber composites, Polym. Polym. Compos. 31 (2023) 1–14, https://doi.org/10.1177/09673911231171035.

[10] A.A. Abdelsalam, S. Araby, S.H. El-Sabbagh, A. Abdelmoneim, M.A. Hassan, Effect of carbon black loading on mechanical and rheological properties of natural rubber/styrene-butadiene rubber/nitrile butadiene rubber blends, J. Thermoplast. Compos. Mater. 34 (4) (2021) 490–507, https://doi.org/10.1177/0892705719844556.

[11] H. Tan, A.I. Isayev, Comparative study of silica-, nanoclayand carbon black-filled EPDM rubbers, J. Appl. Polym. Sci. 109 (2008) 767–774, https://doi.org/10.1002/app.28130.

[12] D. Bartosik, B. Szadkowski, M. Kusmierek, P. Rybinski, U. Mirkhodzhaev, A. Marzec, Advanced ethylene-propylene-diene (EPDM) rubber composites filled with raw silicon carbide or hybrid systems with different conventional fillers, Polymers 14 (2022) 1383, https://doi.org/10.3390/polym14071383.

[13] I. Surya, N. Hayeemasae, M. Ginting, Cure characteristics, crosslink density and degree of filler dispersion of kaolin-filled natural rubber compounds in the presence of alkanolamide, in: IOP Conf Series: Materials Science and Engineering, 2018, https://doi.org/10.1088/1757-899X/343/1/012009.

[14] L. Sierra, B.L. Lopez, J.L. Guth, Microstructural studies of the interactions in SB rubber and mesoporous silica mixtures, Mater. Res. Innov. 5 (6) (2002) 268–276, https://doi.org/10.1007/s10019-002-0160-z.

[15] G.H. Kim, Y.I. Moon, J.K. Jung, M.C. Choi, J.W. Bae, Influence of carbon black and silica fillers with different concentrations on dielectric relaxation in nitrile butadiene rubber investigated by impedance spectroscopy, Polymers 14 (1) (2022) 155, https://doi.org/10.3390/polym14010155.

[16] T.S. Balakrishnan, M.T.H. Sultan, J. Naveen, F.S. Shahar, M.I. Najeeb, A.U.M. Shah, T. Khan, T.A. Sebaey, Selection of natural fibre for pultruded hybrid synthetic/natural fibre reinforced polymer composites using analytical hierarchy process for structural applications, Polymers 14 (15) (2022) 3178, https://doi.org/10.3390/polym14153178.

[17] G. Mittal, V. Dhand, J.I. Ryu, K.Y. Rhee, H.J. Kim, D.H. Jung, Fabrication of modified MMT/glass/vinylester multiscale composites and their mechanical properties, J. Nanomater. (2015) 506029, https://doi.org/10.1155/2015/506029, 2015.

[18] H.M. Naguib, G. Hou, Vinylester-glass fiber composite for water pipe: processing and effect of fiber direction, Egypt. J. Pet. 32 (2023) 24–30, https://doi.org/10.1016/j.ejpe.2023.08.001.

[19] A. Taherzadeh-Fard, A. Khodadadi, G. Liaghat, X.F. Yao, M.A.Z. Mehrizi, Mechanical properties and energy absorption capacity of chopped fiber reinforced natural rubber, Compos. C-Open 7 (2022) 100237, https://doi.org/10.1016/j.jcomc.2022.100237.

[20] Q. Zhang, Y. Li, P. Zhu, S. Yuan, A study on natural rubber composites reinforced by carbon fiber, IOP Conf. Ser.: Earth Environ. Sci. 508 (2020) 012196, https://doi.org/10.1088/1755-1315/508/1/012196.

[21] A. Vahidifar, E. Esmizadeh, G. Naderi, A. Varvani-Farahani, Ratcheting response of nylon fiber reinforced natural rubber/styrene butadiene rubber composites under uniaxial stress cycles: experimental studies, Fatigue Fract. Engng. Mater. 41 (2) (2018) 348–357, https://doi.org/10.1111/ffe.12684.

[22] M.A. Lopez Manchado, M. Arroyo, Short fibers as reinforcement of rubber compounds, Polym. Compos. 23 (4) (2002) 666–673, https://doi.org/10.1002/pc.10466.

[23] M. Imiela, R. Anyszka, D.M. Bielinski, Z. Pedzich, M. Zarzecka-Napierała, M. Szumera, Effect of carbon fibers on thermal properties and mechanical strength of ceramizable composites based on silicone rubber, J. Therm. Anal. Calorim. 124 (2016) 197–203, https://doi.org/10.1007/s10973-015-5115-x.

[24] M. Şen, D. Aksüt, B. Karaağaç, The effect of ionizing radiation on the temperature scanning stress relaxation properties of nitrile-butadiene rubber elastomers reinforced by lignin, radiation, Phys. Chem. 168 (2020) 108582, https://doi.org/10.1016/j.radphyschem.2019.108582.

[25] N. Vennemann, M. Wu, M. Heinz, Thermoelastic properties and relaxation behavior of S-SBR/silica vulcanizates, Rubber World 246 (6) (2012) 18–23.

[26] S. Sasmaz, B. Karaagac, N. Uyanık, Utilization of chrome-tanned leather wastes in natural rubber and styrene-butadiene rubber blends, J. Mater. Cycles. Waste Manage 21 (1) (2019) 166–175, https://doi.org/10.1007/s10163-018-0775-9.

[27] S.A. El Mogy, N.A. Darwish, A. Awad, Comparative study of the cure characteristics and mechanical properties of natural rubber filled with different calcium carbonate resources, J. Vinyl Addit. Technol. 26 (3) (2020) 309–315, https://doi.org/10.1002/vnl.21745.

[28] M.S. Sobhy, M.T. Tammam, The influence of fiber length and concentration on the physical properties ofwheat husk fibers rubber composites, Int. J. Polym. Sci. (2010) 528173, https://doi.org/10.1155/2010/528173, 2010.

[29] N. Meissner, W.M. Rzymski, Use of short fıbers as a fıller ın rubber compounds, AUTEX Res. J. 13 (2) (2013) 40–43, https://doi.org/10.2478/v10304-012-0025-5.

[30] C.C. Ekwueme, I.O. Igwe, Cure characteristics and mechanical properties of pineapple leaf fibre filled natural rubber, J. Miner. Mater. Charact. Eng. 6 (2018) 601–617, https://doi.org/10.4236/jmmce.2018.66043.

[31] H. Wen, M. Wang, S. Luo, Y. Zhou, T. Liu, Aramid fiber reinforced EPDM microcellular foams: influence of the aramid fiber content on rheological behavior, mechanical properties, thermal properties, and cellular structure, J. Appl. Polym. Sci. 138 (2021) 50531, https://doi.org/10.1002/app.50531.

[32] G. Ahmet, The effect of Cumin Black (Nigella Sativa L.) as bio-based filler on chemical, rheological and mechanical properties of epdm composites, Turk. J. Eng. 7 (4) (2023) 279–285, https://doi.org/10.31127/tuje.1180753.

[33] S.S. Maged, D.E. El-Nashar, N. Maziad, Cure characteristics and physicomechanical properties of calcium carbonate reinforcement rubber composites, Egypt. J. Sol. 26 (1) (2003) 1–18.

[34] W.O. Egbujuo, P.I. Anyanwu, H.C. Obası, Utilization of chitin powder as a filler in natural rubber vulcanizates: in comparison with carbon black filler, Int. Rev. Appl. Sci. Eng. 11 (2020) 43–51, https://doi.org/10.1556/1848.2020.00006.

[35] A. Shamsabadi, A. Farahani, M.M. Shirkavand, M.J. Hafezi, M. Tohidian, Carbon black/ethylene propylene diene monomer (EPDM) rubber as polymer electrolyte membrane fuel cell gaskets: mechanical and chemical assessment, Iran, Polym. J. 33 (2024) 169–183, https://doi.org/10.1007/s13726-023-01239-9.

[36] S. Manjhi, G. Sarkhel, Effect of maleic anhydride grafted ethylene propylene diene monomer (MAH-g-EPDM) on the properties of kaolin reinforced EPDM rubber, J. Appl. Polym. Sci. 119 (4) (2011) 2268–2274, https://doi.org/10.1002/app.33017.

[37] M.D. Stelescu, A. Airinei, A. Bargan, N. Fifere, M. Georgescu, M. Sonmez, M. Nituica, L. Alexandrescu, A. Stefan, Mechanical properties and equilibrium swelling characteristics of some polymer composites based on ethylene propylene diene terpolymer (EPDM) reinforced with hemp fibers, Mater 15 (2022) 6838, https://doi.org/10.3390/ma15196838.

[38] K.P. Sau, T.K. Chaki, D. Khastgir, Carbon fibre filled conductive composites based on nitrile rubber (NBR), ethylene propylene diene rubber (EPDM) and their blend, Polymer 39 (25) (1998) 6461–6471, https://doi.org/10.1016/S0032-3861(97)10188-4.

[39] J. Wang, W. Wu, W. Wang, J. Zhang, Preparation and characterization of hemp hurd powder filled SBR and EPDM elastomers, J. Polym. Res. 18 (2011) 1023–1032, https://doi.org/10.1007/s10965-010-9503-4.

[40] B.N. Yeşil, B. Karaagac, Properties of NR and NR/ENR based rubber compounds reinforced with chopped and sized carbon fiber, Anadolu Univ. J. Sci. Technol. A-Appl. Sci. Eng. 17 (5) (2016) 926–935, https://doi.org/10.18038/aubtda.279860.
[41] I. Surya, N. Hayeemasae, M. Ginting, Cure characteristics, crosslinkdensity and degree of filler dispersion of kaolin-filled natural rubber compounds in the presence of alkanolamide, Mater. Sci. Eng. A. 343 (2018) 012009, https://doi.org/10.1088/1757-899X/343/1/012009.
[42] Y. Xu, W. Ai, J. Zuo, W. Yang, C. Wei, S. Xu, Mesoporous spherical silica filler prepared from coal gasification fine slag for styrene butadiene rubber reinforcement and promoting vulcanization, Polymers 14 (20) (2022) 4427, https://doi.org/10.3390/polym14204427.
[43] S. Singh, P.K. Guchhait, G.G. Bandyopadhyay, T.K. Chaki, Development of polyimide-nanosilica filled EPDM based light rocket motor insulator compound: influence of polyimide-nanosilica loading on thermal, ablation, and mechanical properties, Compos. Pt. A-Appl. Sci. Manuf. 44 (2013) 8–15, https://doi.org/10.1016/j.compositesa.2012.08.016.
[44] Y. Pan, M. Zhang, J. Zhang, X. Zhu, H. Bian, C. Wang, Effect of silane coupling agent on modification of areca fiber/natural latex, Materials 13 (21) (2020) 4896, https://doi.org/10.3390/ma13214896.
[45] J. Gao, J. Mei, H. Xiong, X. Han, Effect of silane coupling agents on structure and properties of carbon fiber/silicon rubber composites ınvestigated by positron annihilation spectroscopy, Molecules. 30 (2025) 1658, https://doi.org/10.3390/molecules30081658.
[46] C. Hayichelaeh, L.A.E.M. Reuvekamp, W.K. Dierkes, A. Blume, J.W. M. Noordermeer, K. Sahakaro, Enhancing the silanization reaction of the silica-silane system by different amines in model and practical silica-filled natural rubber compounds, Polymers 10 (6) (2018) 584, https://doi.org/10.3390/polym10060584.
[47] C. Arslan, M. Dogan, The effects of fiber silane modification on the mechanical performance of chopped basalt fiber/ABS composites, J. Thermoplast. Compos. Mater. 33 (11) (2020) 1449–1465, https://doi.org/10.1177/0892705719829515.
[48] M. Jacob, S. Thomas, K.T. Varughese, Mechanical properties of sisal/oil palm hybrid fiber reinforced natural rubber composites, Compos. Sci. Technol. 64 (7–8) (2004) 955–965, https://doi.org/10.1016/S0266-3538(03)00261-6.
[49] M. Asghar, N. Iqbal, S.S. Iqbal, M. Farooq, T. Jamil, Ablation and thermo-mechanical tailoring of EPDM rubber using carbon fibers, J. Polym. Eng. 36 (7) (2016) 713–726, https://doi.org/10.1515/polyeng-2015-0337.
[50] S. Öncel, T. Ünügül, U. Abacı, B. Karaagac, Coffee grounds as sustainable filler for bio-based rubber composites, Polym. Compos. 45 (14) (2024) 12611–12623, https://doi.org/10.1002/pc.28654.
[51] A.M. Delgado, F. Julián, Q. Tarrés, J.A. Méndez, P. Mutjé, F.X. Espinach, Bio composite from bleached pine fibers reinforced polylactic acid as a replacement of glass fiber reinforced polypropylene, macro and micro-mechanics of the Young's modulus, Compos. B Eng. 125 (2017) 203–210, https://doi.org/10.1016/j.compositesb.2017.05.058.
[52] H. Ismail, M.R. Edyham, B. Wirjosentono, Bamboo fibre filled natural rubber composites: the effects of filler loading and bonding agent, Polym. Test. 21 (2002) 139–144, https://doi.org/10.1016/S0142-9418(01)00060-5.
[53] S. Araby, L. Zhang, H.C. Kuan, J.B. Dai, P. Majewski, J. Ma, A novel approach to electrically and thermally conductive elastomers using graphene, Polymer 54 (14) (2013) 3663–3670, https://doi.org/10.1016/j.polymer.2013.05.014.
[54] A.G. Akulichev, B. Alcock, A.T. Echtermeyer, Elastic recovery after compression in HNBR at low and moderate temperatures: experiment and modelling, Polym. Test. 61 (2017) 46–56, https://doi.org/10.1016/j.polymertesting.2017.05.003.
[55] Z.H. Li, J. Zhang, S.J. Chen, Effects of carbon blacks with various structures on vulcanization and reinforcement of filled ethylene-propylene-diene rubber, Express. Polym. Lett. 2 (10) (2008) 695–704.
[56] S. Vishvanathperumal, G. Anand, Effect of nanosilica on the mechanical properties, compression set, morphology, abrasion and swelling resistance of sulphur cured EPDM/SBR composites, Silicon 14 (2022) 3523–3534, https://doi.org/10.1007/s12633-021-01138-9.
[57] L. Shen, L. Xia, T. Han, H. Wu, S. Guo, Improvement of hardness and compression set properties of EPDM seals with alternating multilayered structure for PEM fuel cells, Int. J. Hydrogen. Energy 41 (2016) 23164–23172, https://doi.org/10.1016/j.ijhydene.2016.11.006.
[58] S. Dhanasekar, S. Baskar, S. Vishvanathperumal, Halloysite nanotubes effect on cure and mechanical properties of EPDM/NBR nanocomposites, J. Inorg. Organomet. Polym. Mater. 33 (10) (2023) 3208–3220, https://doi.org/10.1007/s10904-023-02754-1.
[59] T. Ünügül, B. Karaagac, Vulcanization of chlorinated polyethylene /chloroprene rubber compounds at lower temperatures in the presence of reactive silanes, J. Appl. Polym. Sci. 138 (2021) 50544.
[60] M.G. Hameed, D.J. Mohammed, B.J. Kadhim, N.H. Al-Mutairi, Effect of some fillers on the mechanıcal properties of butyl rubber, Eur. J. Res. Dev. Sustain. EJRDS 5 (01) (2024) 57–61.
[61] S. Samaržija-Jovanovic, V. Jovanovic, G. Markovic, S. Konstantinovic, M. Marinovic-Cincovic, Nanocomposites based on silica-reinforced ethylene-propylene-diene-monomer/acrylonitrile-butadiene rubber blends, Compos. Part B Eng. 42 (2011) 1244–1250, https://doi.org/10.1016/j.compositesb.2011.02.008.
[62] M.M. Eissa, S.H. Botros, M. Diab, E.S. Shafik, N.N. Rozik, Rice husk fibers and their extracted silica as promising bio-based fillers for EPDM/NBR rubber blend vulcanizates, Clean. Technol. Environ. Policy. 25 (2023) 3203–3218, https://doi.org/10.1007/s10098-023-02604-1.
[63] N. Vennemann, K. Bokamp, D. Broker, Crosslink density of peroxide cured TPV, Macromol. Symp. 245-246 (1) (2006) 641–650, https://doi.org/10.1002/masy.200651391.
[64] B. Karaagac, S.C. Cengiz, Identification of temperature scanning stress relaxation behaviors of new grade ethylene propylene diene elastomers, Adv. Polym. Technol. 37 (3) (2018) 3027–3037, https://doi.org/10.1002/adv.21973.